



Orographic effects on the propagation and rainfall modification associated with the 2007–08 Madden–Julian oscillation (MJO) past the New Guinea Highlands

Yuh-Lang Lin¹ · William Agyakwah¹ · Justin G. Riley¹ · Huang-Hsiung Hsu² · Li-Chiang Jiang²

Received: 5 September 2019 / Accepted: 6 July 2020 / Published online: 18 July 2020
© Springer-Verlag GmbH Austria, part of Springer Nature 2020

Abstract

Based on the tropical rainfall measuring mission (TRMM)-measured rainfall and estimated outgoing longwave radiation (OLR) fields, it is found that 2007–08 Madden–Julian Oscillation (MJO07-08) went through blocking, splitting, and merging stages when it passed over the New Guinea Highlands (NGH). The TRMM-estimated OLR fields fail to capture detailed TRMM rainfall field and thus is not suitable to serve as proxy for rainfall, as also found in previous studies. The mechanism of orographic blocking is explained by strong orographic blocking on the incoming, low-Froude number, and moist flow, which belonged to the flow-around regime. This is evidenced by estimating the Froude number by upstream soundings. The strong blocking forced the flow to go around the mountains on NGH, leading to the splitting of flow and MJO precipitating system and the merging at the southeast tip of New Guinea. Orographic, MJO, and cyclone clouds were shown in both observed and model-simulated results. The major differences of the model-simulated and TRMM-measured precipitation are as follows: (a) the model-simulated rainfall area is much larger than that covered by the observed rainfall and (b) even though they both show comparable maximum rainfall rate, the rainfall estimated by TRMM reveals more localized rainfall spots, which is unexpected since the WRF simulation uses a relatively fine resolution (5 km). In summary, during the blocking stage, the mountains have slowed down the MJO propagation and increased the rainfall amount upstream of the local mountains, while during the splitting and merging stages, the mountains have made significant impacts on the MJO rainfall distribution.

1 Introduction

Since the 1980s, the Madden–Julian Oscillation (MJO) has received considerable attention in part due to its impact on weather systems around the globe and thus plays a key role in intra-seasonal prediction (e.g., Monier et al. 2010). In particular, when an MJO passes over the Maritime Continent (denoted as MC hereafter), its propagation and rainfall are strongly influenced by orography (e.g., Hsu and Lee 2005; Inness and Slingo 2006; Wu and Hsu 2009; Tseng et al.

2017). Specifically, the MJO is often blocked and weakened, occasionally breaks down and ceases to exist, which is often called “the barrier effect of the MC” (e.g., Inness and Slingo 2006; Kim et al. 2017; Zhang and Ling 2017; Ling et al. 2019). In studying MJO propagating across the MC (MJO-C) and those blocked by the MC (MJO-B), Zhang and Ling (2017) found that MJO-C’s rainfall is much higher over the sea than over the land, whereas unlike MJO-C, MJO-B’s rainfall over the sea is never dominant, which suggests that inhibiting convective development over the sea could be a possible mechanism for the barrier effect of the MC. Ling et al. (2019) investigated the effect of diurnal cycle in land convection on the propagation of the MJO over the MC using satellite observations, which supports the MARitime Continent Convective diurnal Cycle (MACCC) mechanism, i.e., the diurnal cycle in land convection acts as an intrinsic barrier effect on MJO propagation over the MC. However, it remains unclear whether the weakened convection over the land is due to the MACCC or the convective clouds of the MJO being forced to go around, instead of go over, the mountainous islands of MC. In this study, we are particularly

Responsible Editor: Emilia Kyung Jin.

✉ Yuh-Lang Lin
ylin@ncat.edu

¹ Department of Physics and Applied Science and Technology Ph.D. Program, North Carolina A&T State University, 302H Gibbs Hall, 1601 E. Market Street, Greensboro, NC 27411, USA

² Research Center for Environmental Changes, Academia Sinica, Taipei, Taiwan

interested in examining the mechanism of orographic blocking of NGH on the MJO which passed over New Guinea in the winter of 2007–08 (MJO07-08).

Figure 1 shows that the MJO, which was characterized by negative Outgoing Longwave Radiation (OLR) anomalies, was weakened when it passed over the MC, mainly due to the MC topography (Hsu and Lee 2005). Hsu and Lee (2005) proposed that lifting and frictional effects caused by the mountains and land-sea contrast in the MC help induce a near-surface moisture convergence to the east of that topography where new deep convection develops. Due to the development of new deep convection on the lee side of the MC, the MJO appears to be jumping from the upstream of the mountains of the MC over to the lee side (Figs. 1 and 2). The mesoscale processes of the MJO propagation over the mountains and the associated rainfall modification, however, remains unclear and needs to be further investigated.

Based on the analyses of the OLR and the 40 yr European Centre for Medium-Range Weather Forecasts (ECMWF) Re-Analysis (ERA-40) datasets, Wu and Hsu (2009) found that when an MJO passes over the MC during boreal winter, subsequent deep convection and near-surface wind anomalies tend to move around mountainous islands, which was resulted from flow splitting around elongated mountainous islands, such as New Guinea Highland (NGH hereafter; Fig. 2). Orographic blocking may force the incoming three-dimensional flow to go over or go around the mountains, depending upon whether there is enough kinetic energy to be converted to potential energy to climb over the obstacle or not, which are called flow-over regime and flow-around regimes, respectively (Smolarkiewickz and Rotunno 1989). These flow regimes are distinguished by the Froude number,

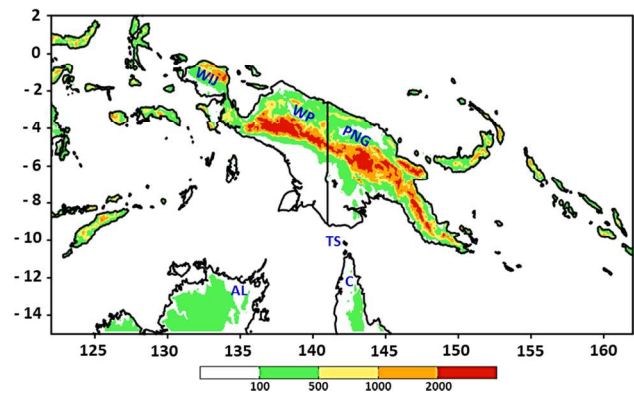
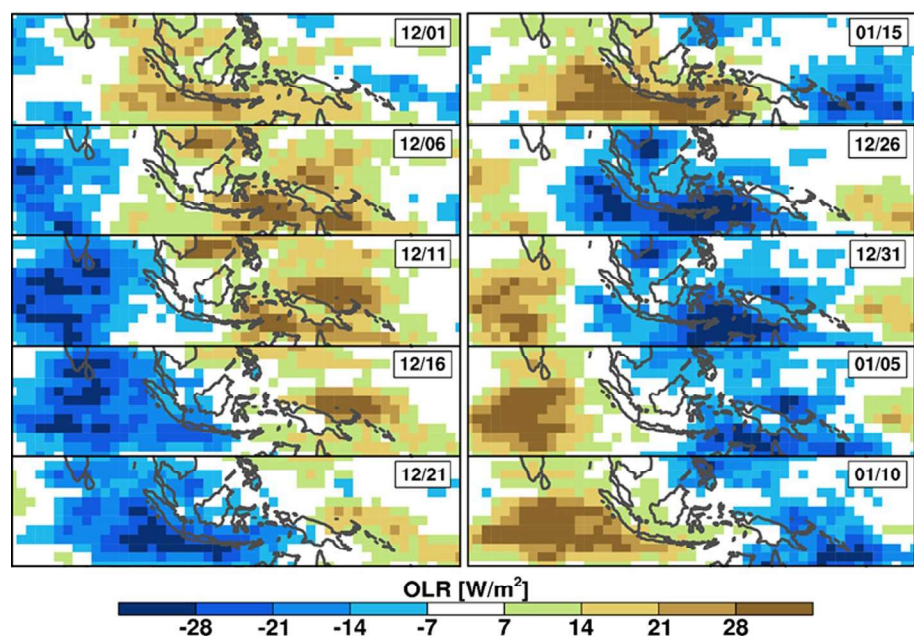


Fig. 2 (Topography) The model domain and topography of New Guinea Highland (NGH), which extends from northwest of New Guinea to the southeast with the highest peak of 4884 m. The terrain height is in m. The topography of regions denoted in this domain are: WP West Irian Jaya (northwest peninsula of the West Papua), PNG Papua New Guinea, AL The Arnhem Land of Australia, C Cape York Peninsula of Australia, TS The Torres Strait

which will be defined and discussed in Sect. 3.2, associated with the upstream flow. The Froude number argument will be applied in this study to investigate the blocking mechanism. Wu and Hsu (2009) found that splitting of flow and precipitating system upstream tend to produce mountain wave-like structures over high mountains in Sumatra, Sulawesi, New Guinea etc. and generate distinctive vorticity and convergence fields on the lee of the mountains. Based on their data analysis, Wu and Hsu (2009) proposed that resolving the detailed topographic effects may play a significant role in simulating realistic characteristics of the MJO passing over the MC.

Fig. 1 (OLR Anomaly) A Hovmöller diagram of 30- to 60-day filtered OLR anomalies (in W m^{-2}) in between 15°N and 15°S everyday from 12/1/07 to 1/10/08



In this study, we are particularly interested in investigating the barrier effects of NGH on the MJO that passed over the NGH during the period of 30 Dec 2007—5 Jan 2008, approximately, which is named as MJO07-08 earlier in this section. The MJO07-08 formed over the Indian Ocean around 12/1/07 (Fig. 1), which approached the MC around 12/11/07. It was then blocked by the Sumatra mountains around 12/21/07; thus, it was forced to go around the island along the southern coast. Around 12/26/07, MJO07-08 split into two parts: one remained upstream of the Sumatra mountains, while the other one continues moving to the Java and upstream of New Guinea. It approached New Guinea around 12/31/07 and appeared to pass over New Guinea during the period of 12/31/07—1/5/08. The MJO convection was weakened significantly when it was passing over the NGH, which might be due to significant blocking. The detailed features of the MJO were still unclear from the OLR analysis (Fig. 1), which is part of the reason we plan to study it using the WRF model. After 1/5/08, the split MJO appeared to merge together and continued propagating downstream to the northern West Pacific Ocean.

Based on the analyses of the Climate Forecast System Re-analysis (CFSR) and National Centers for Environmental Prediction Re-analysis 2 (NCEP R2) data sets, Jiang (2012) found that during the passage of MJO07-08 over the NGH, (1) the westward tilting of vertical circulation with height was much more evident, (2) strong downward motion and moisture divergence was found on the windward side of Sumatra and New Guinea, which were associated with anomalous positive diabatic heating. In addition, an upward motion occurred on the lee side of New Guinea, and (3) vorticity dipoles occurred near the coastline and mountain slopes. Although Wu and Hsu (2009) and Jiang (2012) have helped our understanding of orographic effects associated with NGH on MJO propagation and rainfall during the passage of MJO over the NGH, the proposed mechanisms can be further tested and understood by performing numerical simulations.

Due to the limitation of global model re-analysis data in spatial and temporal resolutions, some detailed dynamics of orographic effects on MJO propagation, such as blocking effects on MJO movement (go over or go around the NGH), propagation speed, structure (maintaining as one system or split), and rainfall distribution, might be overlooked. Some global model simulations did use finer resolution to simulate MJO propagation; however, it is well known that neither the global climate or general circulation models nor downscaled regional climate models are able to accurately represent the temporal variation of MJO in their modeling system, especially over the mountainous areas (e.g., Inness and Slingo 2006; Wu and Hsu 2009; Tseng et al. 2017). To deal with the above problems, we propose to perform real-case mesoscale simulations of the MJO07-08 passing over the NGH

to ascertain the impact orography has on MJO's propagation and rainfall modification. The numerical model we will be using is the WRF model with relatively finer resolution to simulate the convective systems associated with MJO07-08 and compare the results with observations and global re-analysis data. Since MC is composed of a number of mountainous islands (e.g., Sumatra, Java, Borneo, Sulawesi, and New Guinea), which includes a number of complicated physical processes, it is important to understand the propagation and rainfall modification mechanisms associated with an MJO passing over individual mesoscale mountains, such as the NGH.

In this study, we plan to adopt the Weather Research and Forecasting (WRF) model (Skamarock et al. 2008) to simulate the passage of the MJO07-08 over the NGH to help understand the orographic effect on MJO propagation and rainfall modification with a relatively finer horizontal resolution, which can resolve mesoscale features of the topography. The rest of the paper is organized as follows. Section 2 describes the WRF model and experimental design, Sect. 3 provides the general propagation and rainfall characteristics of the MJO07-08 past the MC, Sect. 4 presents and analyzes the WRF-simulated results, and Sect. 5 provides a concluding remark.

2 Model description, experimental design, and the selection of MJO case

The WRF model version 3.6.1 (Skamarock et al. 2008) was adopted for the numerical simulations. The WRF model is a numerical weather prediction system developed to help with both atmospheric research and operational forecasting, which is a three-dimensional, non-hydrostatic, fully compressible model using terrain-following pressure (σ - p) coordinates. The governing equations of the WRF model are written in flux form with conserved mass and dry entropy.

For the mesoscale simulations performed in this study, we only focus on New Guinea, the foremost east and largest island of the MC, and its surrounding areas. Only one domain is designed for our mesoscale simulations, which is from the southwest corner (122°E, -15°S) to northeast corner (162°E, 2°N) consisting of 887 × 376 horizontal grid points with 5 km horizontal grid resolution, 32 vertically stretched grid levels, and 30 s time interval. The domain and NGH terrain are shown in Fig. 2. The domain is designed so that the MJO07-08 and the NGH are well resolved and the orographic impacts on the MJO can be well simulated as it propagated eastward across the mountains.

The physics parameterization schemes chosen for the simulations are as follows: (a) cumulus: Grell 3D, (b) microphysics: WSM6 (Hong and Lim 2006), (c) planetary boundary layer: YSU, (d) surface layer: Monin-Obukov,

(e) longwave radiation: RRTM, and (f) shortwave radiation: RRTMG. Details of these schemes can be found in the WRF user's manual (Skamarock et al. 2008). Unlike global model simulations, the combination of the domain, grid resolution, and physics parameterization schemes allows us to study mesoscale dynamics associated with the passage of the MJO07-08 over the NGH. Note that since some meso- γ (2–20 km) scale convective thunderstorms or systems embedded in MJO cannot be well resolved by 5 km grids, we need to activate the cumulus, in addition to the bulk microphysics parameterizations, to avoid the accumulation of energy at grid points through energy downscale cascading. This is the fuzzy, not-well-defined area, which is often referred to as the “no-man's land,” where neither cumulus parameterization nor microphysical parameterization scheme is dominative.

The WRF-simulated results will be verified by the tropical rainfall measuring mission (TRMM) 3B42 Version 7 data, the NOAA-Interpolated OLR data, and wind vectors data. For the TRMM data, the temporal resolution used is 3 hourly data from 12/30/07 to 1/4/08. Its spatial resolution is 0.25° latitude–longitude grid. For the NOAA-Interpolated OLR, the temporal resolution used is daily data from 12/30/07 to 1/4/08. Its spatial resolution is 2.5° latitude–longitude grid.

When the MJO07-08 passed over the NGH during the period of 12/30/07–1/4/08 is chosen for the study because it is considered as a strong MJO event (Jiang 2012). The mesoscale simulation is initiated with the ECMWF interim data at 0000 UTC. As normally adopted for regional numerical simulations, the boundary conditions are updated by this re-analysis data. The simulation period for the domain is 6 days (12/29/00Z/07–1/4/00Z/08), which was the time the MJO was seen passing over the NGH (Figs. 1, 2, 3, 4, 5, 6), in addition.

3 Observational data analysis of MJO07-08 passing over the New Guinea Highlands (NGH)

3.1 Propagation and rainfall modification by the NGH mountains

The austral summer of 2007–08 was a very active season for strong MJO activity. In the first week of December 2007, the first band of convective clouds associated with the MJO was over the equatorial Indian Ocean as revealed by the OLR fields (12/01/07 and 12/06/07 of Fig. 1; Gottschalck

Fig. 3 (TRMM OLR) Observed mean OLR (w/m^2) from 12/30/00Z/2007 to 1/4/00Z/2008 (TRMM 3B42 data). The local time is 12/30/10L/2007–1/4/10L/2008. It appears that there are three stages during the passage of the MJO over the NGH: (a, b) blocking stage, (c, d) splitting stage, and (e, f) merging stage. The local time is 10 am

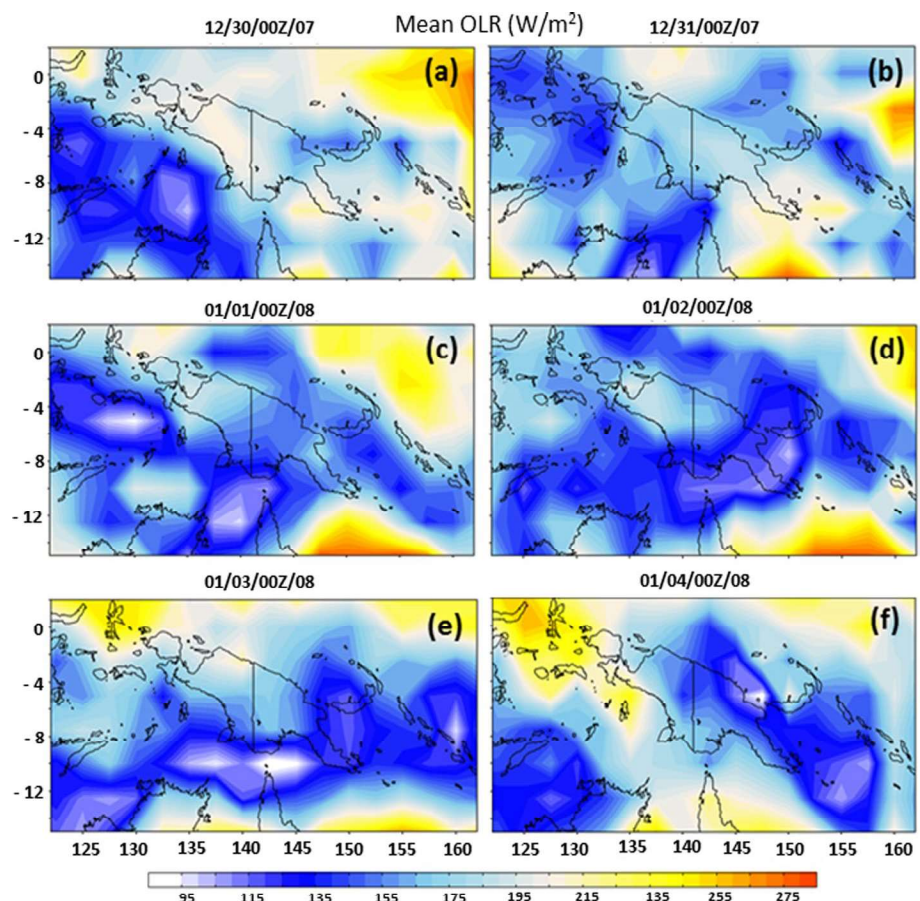
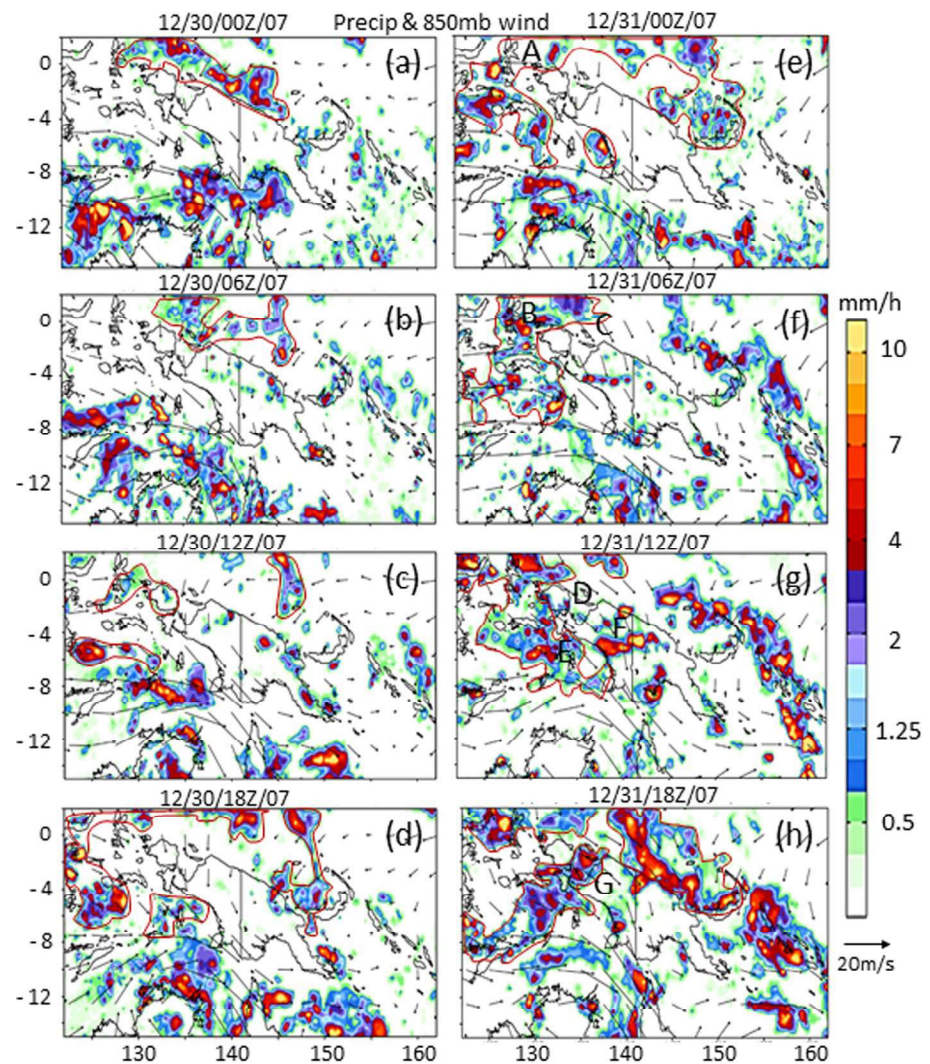


Fig. 4 (TRMM Rain—Blocking Stage) Observed precipitation (mm) and 850 mb winds (m/s) from TRMM and NCEP/NCAR Re-analysis 1 datasets, respectively, for 12/30/00Z/07–12/31/18Z/07 (12/30/10L/2007–1/1/04L/08) during the blocking stage. The solid red contours denote areas with heavy precipitation produced by the convective system associated with the MJO07-08. The local time is 10 am. The letters A-G in (e)–(h) are denoted for different processes associated with orographic blocking, which are explained along with discussions of Fig. 4e–h in Sect. 3

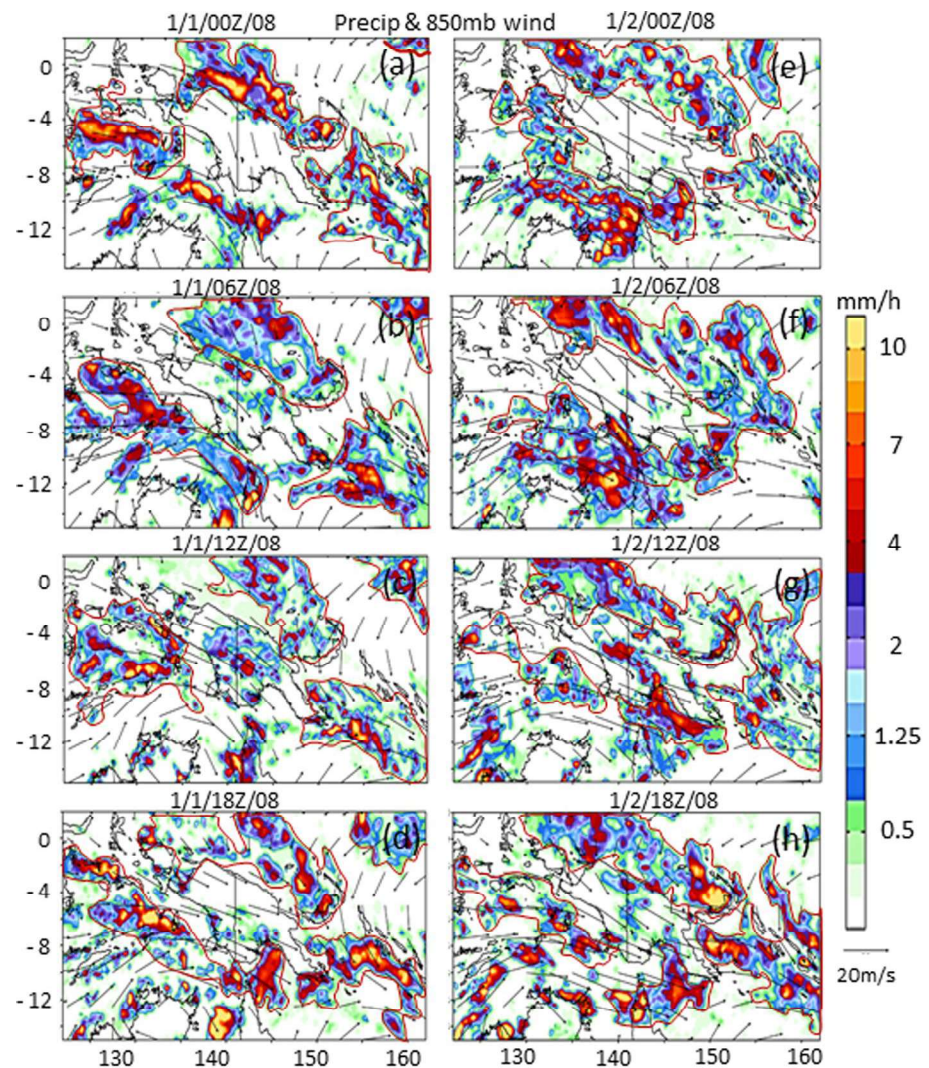


et al. 2008; Tseng et al. 2017). It then propagated eastward reaching the Sumatra around Dec. 11 and was blocked by the mountains over the island in the next two weeks (12/11–12/26/07). Due to orographic blocking, the majority of the convective systems associated with the MJO was forced to move southeastward along the southwest coast of Sumatra (12/16–12/21/07). From 12/21 to 12/26/07, the MJO split into two systems: one system remained to the northwestern coast of the Sumatra, while the other system propagated to the southeast coast. During the period of 12/26–1/31, the northwestern system weakened and then disappeared. From the OLR fields presented in Fig. 1, it is unclear whether the northwestern system was totally diminished due to strong blocking or just stalled in the lower layer, while the convective system in the upper layer continued to propagate southeastward and then merged with the southeastern system vertically as a system at the southeastern corner of Sumatra on 12/31/07 approximately. The latter process is analogous to the discontinuous track experienced

by weak typhoons passing over Taiwan's Central Mountain Range (e.g., Chang 1982; Lin et al. 2016; Lin 2007).

From approximately 12/31/07 or slightly earlier till around 1/5/08, the MJO has left Sumatra completely (Fig. 1). In the meantime, it was passing over New Guinea. While passing over New Guinea, it appeared to split into two systems, too, although they seemed to pass over the island along northeast and southwest coasts, respectively. On 1/10/08, the MJO re-appeared to the southeast of New Guinea. Thus, the MJO passed over New Guinea occurred approximately from 12/31/07 to 1/5/08. From 12/21/07 to 1/10/08, the MJO appeared to jump over the MC, instead of moving smoothly over it. In this study, we will focus on the propagation of MJO07-08 over New Guinea or NGH. In order to examine the details of the propagation of MJO07-08 passing over the NGH, mesoscale analyses are performed using more detailed observation of OLR and rainfall from TRMM 3B42 data (Simpson et al. 1996; Huffman et al. 2007) and 850mb wind fields from NCEP/National Center for Atmospheric

Fig. 5 (TRMM Rain – Splitting Stage) Same as Fig. 4 except from 1/1/00Z/08 to 1/2/18Z/08 (1/1/10L/08–1/3/04L/08) (TRMM 3B42 data) during the splitting stage



Research (NCAR) Re-analysis 1 dataset (Kalnay et al. 1996). Note that the OLR is used in this study to identify the main MJO-convective envelope and surrounding cirrus clouds (precipitating and non-precipitating clouds), instead of using it as a proxy of the rainfall over the land, since it has been found that OLR is not a good proxy for precipitation over land of the MC (e.g., Matthews et al. 2013; Rauniyar and Walsh 2013; Peatman 2014), which includes New Guinea. In addition, it was found that in steep mountain areas of the NGH.

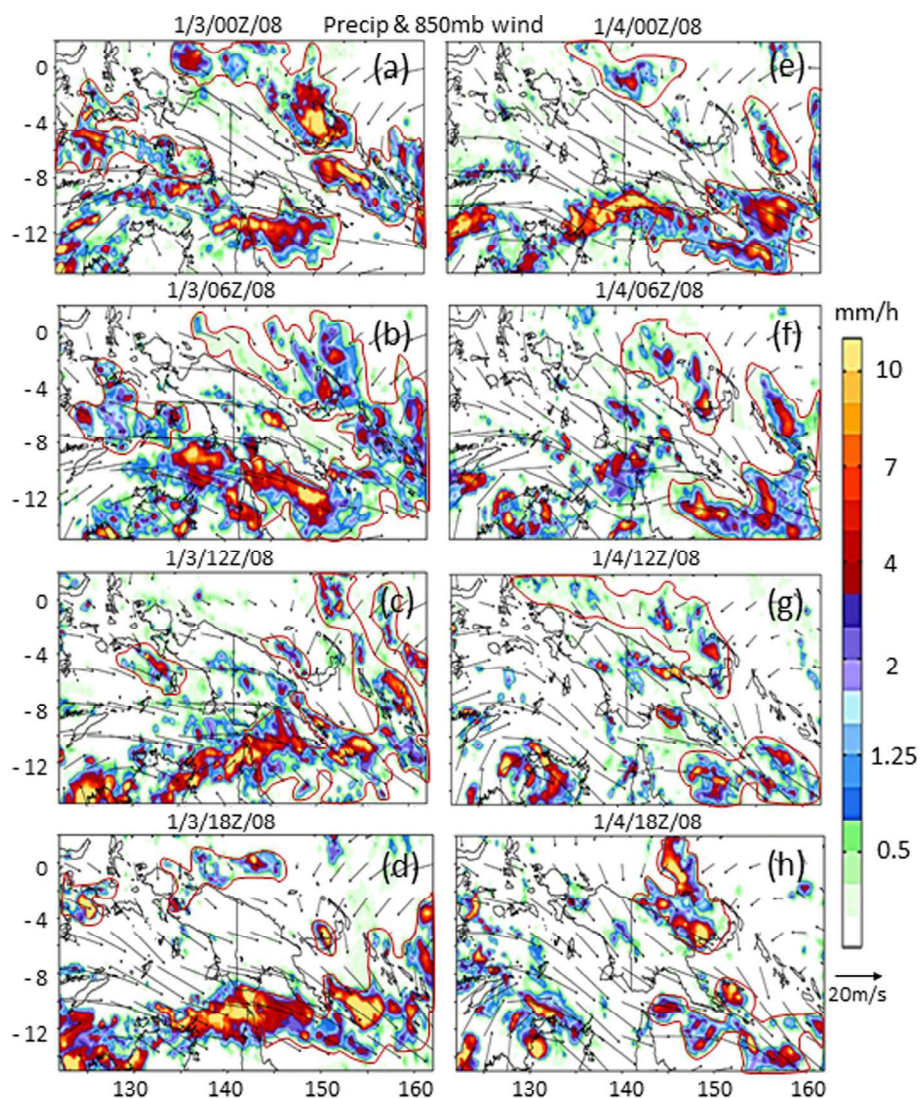
(a) Blocking of the MJO precipitating systems

Based on the observed OLR fields from TRMM data, it appears that the MJO07-08 has gone through roughly three distinctive stages when it passed over the NGH (Fig. 3). At 12/30/00Z/07, the southern MJO reached the western New Guinea and was blocked and stalled on the southwestern side of the northwestern NGH (Fig. 3a). The blocking was clearer on the next day at

12/31/00Z/07 (Fig. 3b). The cloud was located exactly to the upstream of the northwest peninsula of New Guinea (West Irian Jaya—WIJ in Fig. 2). This period of 12/30—12/31/07 may be named the *Blocking Stage*.

The blocking stage identified approximately from the TRMM-estimated OLR fields can be verified much more accurately and in detail by the TRMM-measured precipitation fields (Fig. 4). From 12/30/00Z–12/30/18Z/07, the orographic blocking on the southern system of the MJO clouds (Fig. 3a) can be seen clearly from the precipitation fields to the southwest of the NGH (Fig. 4a–d). Note that the rainfall to the north of the northeast coast of NGH at 12/30/00Z/07 was northern system of the MJO after it passed over the Sumatra (Day 12/31, Fig. 1), which was not detected by the OLR field at this time (Fig. 3a), and continued to propagate along the northeast coast of New Guinea for the rest of the day (12/30/06Z–12/30/18Z (Fig. 4b–d). From 12/31/00Z to

Fig. 6 (TRMM Rain—Merging Stage) Same as Fig. 4 except from 1/3/00Z/08 to 1/4/18Z/08 (1/3/10L/08–1/5/04L/08) (TRMM 3B42 data) during the merging stage



12/31/18Z/07, the blocking of the MJO clouds (Fig. 3b) and precipitation (Fig. 4e–h) in the western portion of the mountains of NGH was much stronger.

During the blocking stage, it appears that the incoming MJO went through three processes:

(1) During 12/31/00Z–12/31/06Z/07, the moist flow with embedded precipitating system of MJO0708 around A in Fig. 4e impinged on the mountains of *northwest peninsula* of the West Papua (WIJ in Fig. 2), which produced more rainfall over the ocean just upstream of the northwest peninsula (B in Fig. 4f). The blocking is associated with low-Froude number flow, which will be verified with the flow parameters and discussed later in Sect. 3.2.

(2) In the meantime, part of the incoming moist flow was forced to go around the northwest peninsula (WIJ) (C in Fig. 4f) due to strong blocking associated with small Froude number flow passing over a three-

dimensional mountain, which will be illustrated later in Sect. 3.2.

(3) During 12/31/12Z–12/31/18Z/07, the moist flow around D in Fig. 4g impinged on the mountains of West Papua (Fig. 2), which generated heavy rain and/or enhanced the pre-existing rain associated with MJO0708 upstream (northwest) of West Papua, as denoted by G in Fig. 4g. Note that at 12/31/18Z, there was a significant amount of rainfall produced in between the northwest peninsula (WIJ) and the main island of New Guinea (rainband G in Fig. 4h). Rainband G was composed of the MJO-convective rain blocked by the mountains in northwestern NGH in the northeast part and enhanced by the interaction with the rainband of Cyclone Helen in the southwest part of the rainband G, respectively.

(b) Splitting of the MJO precipitating system

During the period of 1/1–1/2/08, it can be seen from the OLR fields (Fig. 3c–d) that the MJO precipitating system approximately split into two systems with the northern and southern systems moving along the northeast and southwest coasts of NGH, respectively, toward the southeastern tip of New Guinea. Both the northern and southern systems of the MJO precipitating system then propagated to the lee side (southeastern tip) of the mountains at a later time. Note that the split MJO precipitating systems were going around the New Guinea during this *Splitting Stage* (1/1/00Z–1/2/18Z/08; Fig. 5a–h).

Note that during both blocking and splitting stages, there was a lack of rainfall over New Guinea except at 12/31/12Z/07 near F and at 12/31/18Z/07 over the northeastern part of rainband G. Diurnally forced rainfall over islands of MC was often observed for MJOs blocked by MC (e.g., MJO-B classified by Zhang and Ling 2017) and on New Guinea during the passage of MJO (Matthews et al. 2013). We suspect that the lack of rainfall over New Guinea might be due to the coarse resolution of the TRMM-observed data. This will be examined by the numerically simulated results in Sect. 4.

(c) Merging of the MJO precipitating systems

Based on the TRMM-estimated OLR fields during 1/3/00Z–1/4/00Z/08 (Fig. 3e, f), the split MJO cloud systems were merging into one system around the southeastern tip, which may be named *Merging Stage*. In the beginning of this merging stage, the northern system of the MJO continued moving southeastward toward the southeastern tip of New Guinea (Fig. 6a–d) and merged with the southern system. The southern system moved southeastward along the southwest coast of New Guinea in the beginning (Fig. 6a–b), but then strengthened and started to move eastward (Fig. 6c–d), which may be explained by the interaction with Cyclone Helen. At 1/4/18Z/08, these two MJO systems merged at the southeastern tip of New Guinea.

Similar to the blocking and splitting stages, there was a lack of rainfall on New Guinea. This will be investigated by the model-simulated results in Sect. 4.

3.2 Mechanism of orographic blocking on the MJO07-08

As mentioned in the introduction, the three-dimensional orographic blocking may lead to flow-over and flow-around regimes, depending on the Froude number of the upstream incoming flow. The lower the moist Froude number, the stronger is the blocking, which may lead to flow splitting. When blocking is weak, the incoming flow is able to pass over it, which is called *flow-over regime*. On

the other hand, when blocking is strong, the incoming flow is the lack of kinetic energy to pass over the barrier, causing the flow to be blocked leading to split, which is called *flow-around regime* (Smolarkiewicz and Rotunno 1989). The flow-over and flow-around regimes are mainly controlled by two non-dimensional parameters, i.e., Froude number ($F = U/Nh$) and aspect ratio (b/a) of the mountain scales in along (a) and perpendicular (b) to the basic flow direction, where U is the basic flow speed, N is the Brunt-Vaisala frequency, and h is the mountain height (e.g., Smith 1989; Epifano 2003; Lin 2007). For example, a dry atmospheric flow ($F, b/a$) = (0.66, 1) belongs to the *flow-over regime*, while ($F, b/a$) = (0.22, 1) belongs to the *flow-around regime* (Smolarkiewicz and Rotunno 1989). Based on Fig. 5.22 of Lin (2007), a rough estimate for a dry airflow impinging on a mountain with an aspect ratio of $b/a = 0.5$ requires $F = 0.45$ to make a flow split or go around flow regime.

For moist flow, it is more suitable to use the moist Froude number, which is defined as $F_w = U/N_w h$, where N_w is the unsaturated Brunt-Vaisala frequency (e.g., Chen and Lin 2005; Lin 2007) of the upstream incoming flow. In idealized simulations of conditionally unstable flow impinging on a two-dimensional, mesoscale mountain, Chu and Lin (2000) found that the precipitation distribution and propagation of orographically induced precipitating systems vary with the moist Froude number. The unsaturated Brunt-Vaisala frequency (N_w) is defined by Emanuel (1994) as

$$N_w^2 = \frac{g}{\theta_v} \frac{\partial \theta_v}{\partial z} \quad (1)$$

where g is the gravitational acceleration and θ_v is the virtual potential temperature, which can be calculated by (Glickman 2000)

$$\theta_v = \theta(1 + 0.61q_v - q_L) \quad (2)$$

where θ is the actual potential temperature and q_v and q_L are the mixing ratios of water vapor and liquid water, respectively.

As discussed above in Sect. 3.1(a), during the blocking stage (12/30–12/31/07), the incoming flow with embedded precipitating systems of MJO07-08 was blocked more severely twice: (1) during 12/31/06Z–12/31/06Z, the flow around A in Fig. 4e impinged on the mountains of northwest peninsula (WIJ in Fig. 2) around 12/31/06Z (denoted by B in Fig. 4f), and (2) during 12/31/12Z–12/31/18Z/07, the flow around D in Fig. 4g impinged on the mountains of West Papua (Fig. 2) around 12/31/18Z/07 (denoted by G in Fig. 4h). Both processes generated rain and/or enhanced the pre-existing rain associated with MJO07-08 upstream of the mountains on northwestern peninsula (WIJ) and on the West Papua, respectively. Both blocking events were

associated with flow going around the mountains (Fig. 4f, h, respectively).

The moist Froude numbers, F_{w1} and F_{w2} , are estimated by 4 WRF-simulated upstream soundings around A in Fig. 4a, d in Fig. 4g, respectively. The flow variables in the lower layer (1000–850 mb) are pressure (p), temperature (T), dew point (T_d), mixing ratios of water vapor (q_v), cloud water (q_c), rain water (q_r), and potential temperature (θ). Then, the density (ρ) is calculated by the equation of state, and virtual potential temperature (θ_v) and unsaturated Brunt-Vaisala frequency (N_w) are calculated from Eqs. (2) and (1), respectively. At last, the moist Froude number (F_{w1}) for each sounding is calculated by $U_1/N_{w1}h$ with N_{w1} calculated from Eq. (1), an averaged $U_1 = 5.6 \text{ m s}^{-1}$ estimated from the surrounding 4 soundings around A (Fig. 4e) and a rough mountain height of 2 km is used. The F_{w1} is averaged from the 4 F_{w1} 's calculated from each sounding surrounding A, which has a value of 0.3. The averaged F_{w2} is calculated in the same way, which gives a value of 0.217, except with $U_1 = 7.1 \text{ m s}^{-1}$ and $h = 3 \text{ km}$. The detailed data can be found from Tables 1 and 2. Both estimated F_{w1} (0.3) and F_{w1} (0.217) indicate that the moist flow impinging on the northwest peninsula (WIJ) and northwestern tip of West Papua belong to the flow-around regime due to strong blocking; thus, the flow was blocked and forced to go around the

mountains in respective mountain regions, which also forced the MJO precipitating systems to split leading to the *splitting stage*.

The MJO propagation over the NGH and their associated rainfall modification by the mountains will be verified and further investigated in detail by the WRF-simulated results in the next section.

4 Numerical modeling simulations of the propagation and rainfall modification of MJO07-08 passing over the New Guinea Highlands (NGH)

In this section, the WRF-simulated results are verified by TRMM-estimated OLR and measured rainfall, as presented in Sect. 3, and are used to investigate the orographic effects on the propagation and rainfall modification of the MJO during its passage over the NGH. In particular, the mesoscale characteristics and temporal evolution of the MJO will further be investigated in detail by the WRF-simulated results.

Based on the observational data analyses as discussed in Sect. 3, the propagation of the MJO07-08 over the NGH went through three stages, i.e., the blocking, splitting, and merging stages (Figs. 3, 4, 5, 6). In the following, we

Table 1 Calculation of Moist Froude Number (F_{w1}) from 4 WRF-simulated upstream soundings of West Irian Jaya (WIJ or Northwest Peninsula)

P (mb)	T (°C)	T_d (°C)	q_v (g/kg)	q_c (g/kg)	q_r (g/kg)	θ (K)	ρ	θ_v (K)	N_w (s ⁻¹)	F_{w1}
Sounding 1a: (129.05E, 1.00 N)										
1000	26.9	24.9	19.3	0.0	0.0	301	1.161	305	0.00696	0.402
950	24.9	22.9	17.4	0.0	0.0	302	1.111	305	0.00953	0.294
900	22.9	16.9	13.5	0.0	0.0	304	1.059	307	0.01303	0.215
850	18.9	12.9	11.0	0.0	0.0	307	1.014	309	0.00735	0.381
Sounding 1b: (129.33E, 1.00 N)										
1000	26.9	24.9	20.0	0.0	0.0	300	1.161	304	0.0078	0.360
950	24.9	22.9	19.0	0.0205	0.0	301	1.111	304	0.0122	0.230
900	22.9	16.9	14.0	0.0	0.0	304	1.059	307	0.0098	0.285
850	18.9	12.9	11.0	0.0	0.0	306	1.014	308	0.0110	0.254
Sounding 1c: (129.33E, 0.73 N)										
1000	28.0	25.0	19.5	0.0	0.0	302	1.157	306	0.0120	0.233
950	24.0	22.0	18.5	0.0	0.0	302	1.114	305	0.0119	0.236
900	21.0	18.0	13.0	0.0	0.0	305	1.066	307	0.0108	0.260
850	20.0	12.0	11.5	0.0	0.0	307	1.010	309	0.0072	0.390
Sounding 1d: (129.05E, 0.73 N)										
1000	28.0	24.0	18.5	0.0	0.0	301	1.157	304	0.0073	0.382
950	24.0	20.0	17.0	0.0	0.0	302	1.114	305	0.0127	0.221
900	22.0	16.0	13.0	0.0	0.0	305	1.062	307	0.0107	0.261
850	20.0	14.0	11.5	0.0	0.0	307	1.010	309	0.0072	0.390

$$N_w^2 = \frac{g}{\theta_v} \frac{\partial \theta_v}{\partial z}, g: \text{gravitational acceleration; } \theta_v: \text{virtual potential temperature (see Eq. 2) (1)}$$

$$\theta_v = \theta(1 + 0.61q_v - q_L), q_v: \text{water vapor mixing ratio, } q_L = q_c + q_r \text{ (2)}$$

$$F_{w1} = \frac{U_1}{N_{w1}h_1}, U_1 = 5.6 \text{ ms}^{-1}, h_1 = 2 \text{ km}, N_{w1}: \text{see the table above}$$

$$F_{w1} = 0.300 \text{ averaged from the 4 } F_{w1} \text{'s calculated above}$$

Table 2 Calculation of moist Froude number (F_{w2}) from 4 WRF-simulated upstream soundings of West Papua

P (mb)	T (°C)	T_d (°C)	q_v (g/kg)	q_c (g/kg)	q_r (g/kg)	θ (K)	ρ	θ_v (K)	N_w (s ⁻¹)	F_{w1}
Sounding 2a: (134.00E, 0.00 N)										
1000	28.0	24.0	19.5	0.0	0.0	302	1.157	306	0.0086	0.275
950	24.0	22.0	18.5	0.0	0.0	302	1.114	305	0.0101	0.234
900	22.0	20.0	15.5	0.0	0.0	304	1.062	307	0.0130	0.183
850	18.0	16.0	12.8	0.0	0.0	307	1.017	309	0.0069	0.345
Sounding 2b: (134.00E, 0.00 N)										
1000	28.0	26.0	20.0	0.0	0.0	300	1.157	304	0.0119	0.199
950	24.0	24.0	19.5	0.0100	0.0	302	1.114	306	0.0098	0.241
900	22.0	20.0	16.0	0.0	0.0	304	1.062	307	0.0123	0.192
850	18.0	14.0	12.0	0.0	0.0	307	1.017	309	0.0107	0.220
Sounding 2c: (134.67E, 0.25S)										
1000	28.0	26.0	20.0	0.0	0.0	301.0	1.157	305	0.0078	0.305
950	24.0	24.0	19.0	0.0020	0.0008	302.0	1.114	305	0.0106	0.222
900	22.0	20.0	16.8	0.0	0.0	304.0	1.062	307	0.0093	0.254
850	18.0	16.0	13.0	0.0	0.0	306.0	1.017	308	0.0102	0.232
Sounding 2d: (134.00E, 0.25S)										
1000	28.0	24.0	18.5	0.0	0.0	301	1.157	304	0.0073	0.382
950	24.0	20.0	17.0	0.0	0.0	302	1.114	305	0.0127	0.221
900	22.0	16.0	13.0	0.0	0.0	305	1.062	307	0.0107	0.261
850	20.0	14.0	11.5	0.0	0.0	307	1.010	309	0.0072	0.390

Same as Table 1 except

$$F_{w2} = \frac{U_2}{N_w h_1}, U_2 = 7.1 \text{ ms}^{-1}, h_1 = 3 \text{ km}, N_w: \text{ see above tables}$$

$$F_{w2} = 0.217 \text{ averaged from the 4 } F_{w2} \text{'s calculated above}$$

examine the OLR, precipitation, wind, and cloud fields on various height levels at different stages of the WRF-simulated MJO07-08 when it passed over New Guinea in more detail.

4.1 Blocking stage

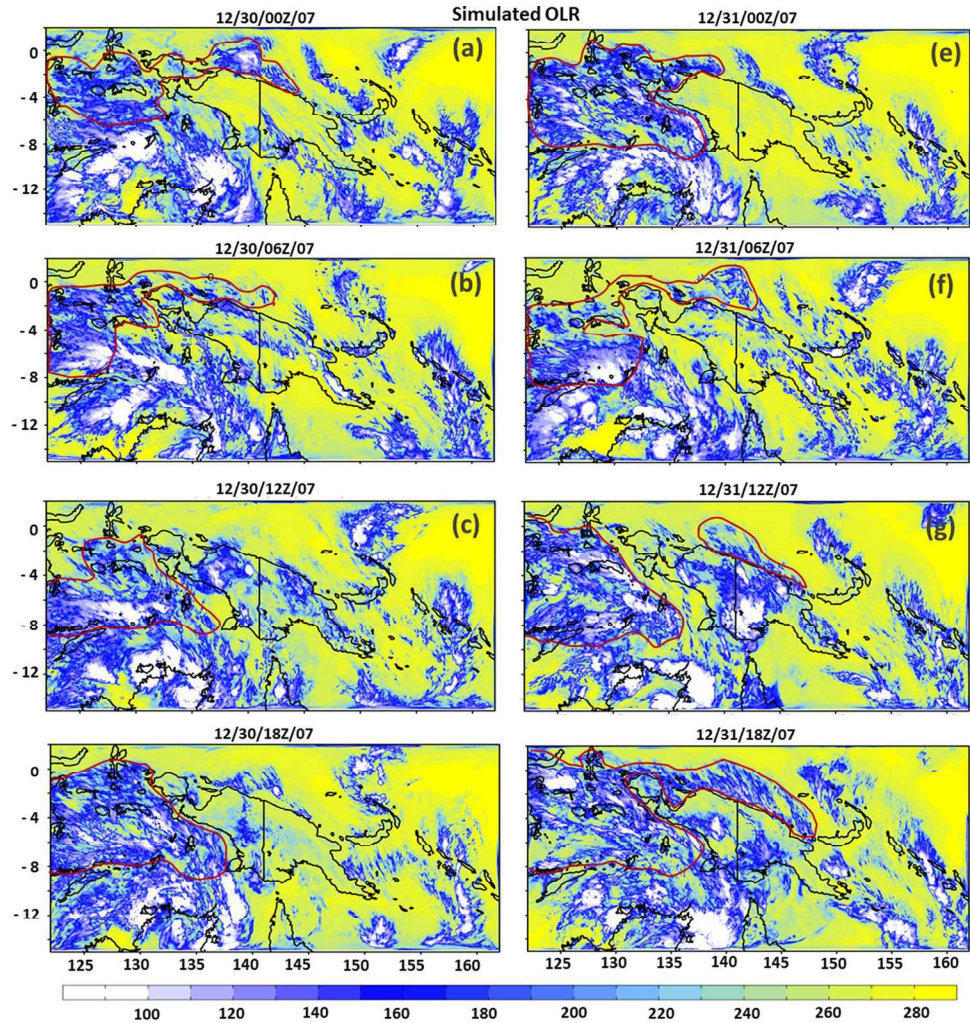
As discussed in Sect. 3, during the period of 12/30 – 12/31/07, the MJO reached the northwestern corner of New Guinea, as can also be seen roughly from 12/31/07 of Figs. 1 and 3a, b. Since the observed OLR does not show the MJO clearly, we will use the observed rainfall as proxy of the MJO precipitating system. However, we are still curious about how well the model-simulated OLR can represent the MJO. Thus, both model-simulated OLR and precipitation fields will be compared to each other and also compared with the observed precipitation fields.

The WRF-simulated OLR fields during the blocking stage (12/30/00Z–12/31/18Z/07) reveal that the MJO began to stall upstream (to the west) of northern West Papua on 12/30 (Fig. 7a–d) and to the northwest of northern West Papua on 12/31 (Fig. 7e–h). Note that there were three types of clouds shown in the model-simulated OLR fields: (i) MJO clouds: mainly over the ocean surrounding the New Guinea during the passage of MJO07-08 over New Guinea, (b) orographic clouds: over land, but concentrated on the

NGH and surrounding areas, peaked at around afternoon and evening (06Z and 12Z; 16L and 22L) in both 12/30 and 12/31 (Fig. 7b–c, f–g) and varied diurnally, and (c) cyclone clouds: high and circular clouds associated with Cyclone Helen, located over ocean in between New Guinea, Arnhem Land (Australia), and Cape York Peninsula (Australia) (see Fig. 2). In addition to the NGH, Cyclone Helen (Wikipedia 2018) appears to also help stall the convective system associated with MJO07-08 to the south of New Guinea. The WRF-simulated OLR fields (Fig. 7) are able to depict major features shown in observed precipitation fields (Fig. 4), compared to the observed OLR (Fig. 3). The lack of detailed rainfall characteristics of the observed rainfall (Fig. 4) appears to be caused by the coarse resolution of the TRMM data, which is not appropriate to serve as proxy of the MJO rainfall, as also found in previous studies (e.g., Matthews et al. 2013; Rauniyar and Walsh 2013; Peatman et al. 2014).

Figure 8 shows the WRF-simulated precipitation fields from 12/30/00Z to 12/31/18Z/07, which are consistent with the observed TRMM precipitation (Fig. 4), but with much more detailed features. All three types of rainfall, i.e., MJO, orographic, and cyclone rainfall, are all well depicted by the WRF-simulated rainfall fields. Especially, the WRF-simulated rainfall fields are able to reveal the orographic blocking reasonably well. For example, Fig. 8a shows that the MJO07-08 began to stall by the

Fig. 7 (WRF OLR-Blocking Stage) WRF-simulated OLR fields for 12/30/00Z/07–18Z/12/31/07 (12/30/10L/07–1/1/04L/08). The solid red contours denote areas with MJO deep convective clouds approximately. The orographic clouds can be seen over land



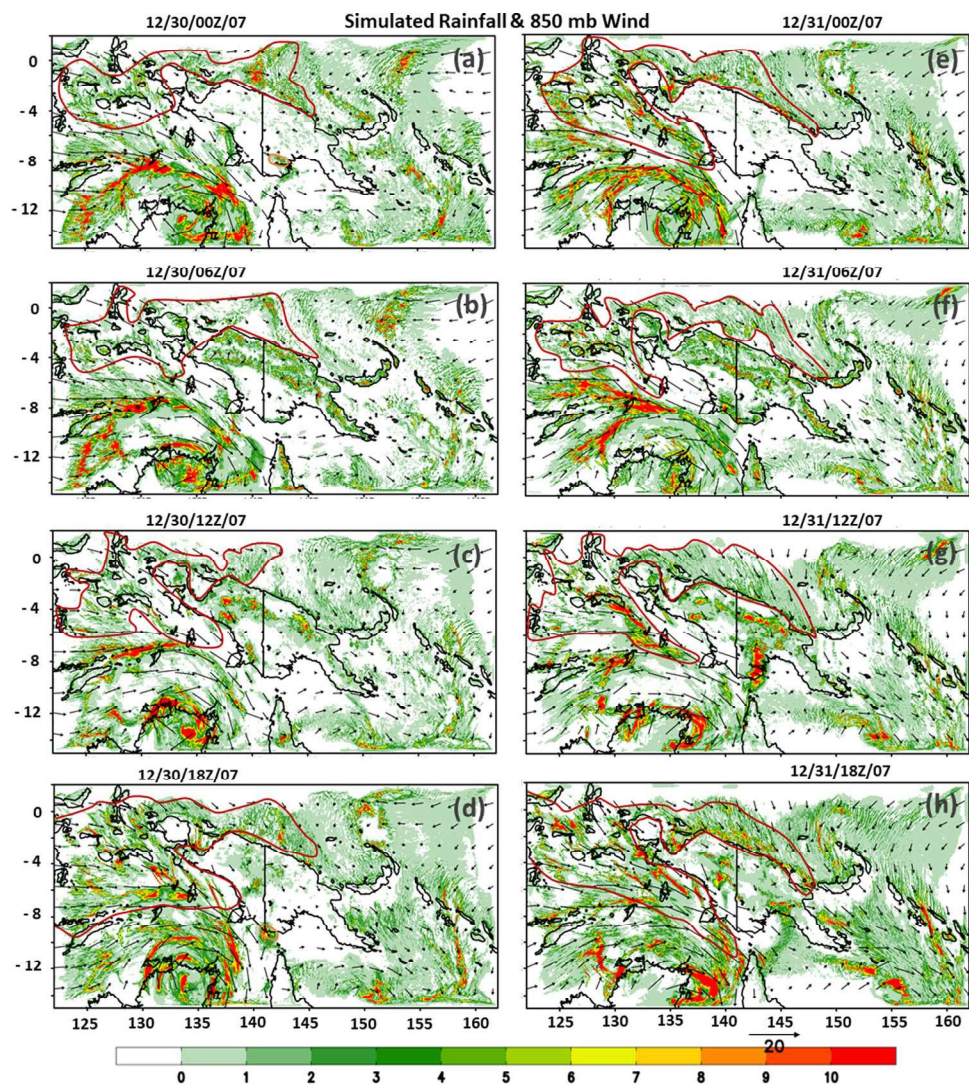
NGH mountains at 12/30/00Z/07 (Fig. 8a), which lasted until 12/31/18Z/07 (Fig. 8b–h), consistent with observations (Fig. 4). The blocking of MJO by the NGH, as discussed in Sect. 3.2, is well depicted from the rainfall accumulation to the upstream of the northwest corner of the NGH. The flow that went around the mountains on the northwest NGH is also shown in the 850 mb wind and precipitation fields during the blocking period and started to split at the end of the blocking period, i.e., 12/31/12Z to 12/31/18Z/07 (Fig. 8g–h). The diurnal variation of the rainfall is much more pronounced, compared to that shown in the WRF-simulated OLR fields (Fig. 7). *The major differences between the WRF-simulated (Fig. 8) and TRMM-measured (Fig. 4) precipitation are as follows:* (a) the model-simulated rainfall area is much larger than that covered by the observed rainfall and (b) even though they both show comparable maximum rainfall rate ($\sim 10 \text{ mm h}^{-1}$), the rainfall estimated by TRMM data reveals more localized rainfall spots, which is unexpected since the WRF simulation uses a relatively fine resolution (5 km).

The blocking effect of the NGH on the rainfall associated with MJO07–08 is further examined by analyzing the three-dimensional wind and total water content fields on 850, 500, and 300 mb surfaces (Fig. 9). At 12/31/00Z/07, one can see that the total water contents or clouds were stalled by the mountains of the NGH on the incoming flow and MJO, i.e., the northwestern corner of the island in the lower troposphere, as shown at 850 mb (Fig. 9c). The middle and upper tropospheric clouds were stronger, as shown at 300 mb and 500 mb (Fig. 9a, b, respectively), than those in the lower troposphere that are associated with anvil clouds associated with convection originating in the lower troposphere. The lack of clouds over New Guinea at this time (12/31/00Z/07) was because it is in the morning (10L), consistent with the rainfall fields (Fig. 8a, e).

4.2 Splitting stage

Based on the TRMM-estimated OLR (Fig. 3c–d) and precipitation (Figs. 4, 5, 6) fields, it can be seen that the MJO after

Fig. 8 (WRF Rain-Blocking Stage) WRF-simulated precipitation (mm) and 850 mb wind (ms^{-1}) fields from 12/30/00Z/07 to 12/31/18Z/07 (12/30/10L/07–1/1/04L/08). The solid red contours denote areas with heavy precipitation associated with the MJO. The orographic precipitation can be seen clearly over land



the blocking stage on the upstream (northwestern corner) of the NGH split into two: one passes along the northeast coast, while the other passes along the southwest side of the NGH. The splitting of the precipitating system (clouds and precipitation) associated with MJO07-08, as discussed in Sect. 3.2, was caused by the low-Froude number moist flow upstream (to the northwest) of the mountains on northwestern New Guinea. The flow belonged to flow-around regime, which forced the flow and the convective system associated with MJO07-08 to be blocked at the northwestern corner of New Guinea and then forced the incoming flow and convective system to split while went around the island.

As discussed in Sect. 3.1, right after the blocking stage, the precipitating system associated with the MJO split into two systems passing over the NGH during the period of 1/1/08–1/2/08 approximately. The northern system propagated along the northeast coast of New Guinea, while the southern system propagated southeastward along the southwest coast. Both precipitating systems of the MJO then

propagated to the lee side (southeastern corner) of the NGH at later time.

Figure 10 shows the WRF-simulated OLR fields from 1/1/00Z/08 to 1/2/18Z/08 (1/1/10L–1/3/04L/08), which represent cloud patterns in more detail, compared to the TRMM-estimated OLR (Fig. 3c, d). Similar to the blocking stage (Fig. 7), we found that (a) the TRMM-estimated OLR was not quite accurate and is not appropriate to serve as proxy of MJO precipitation, and (b) the three types of clouds associated with the MJO, orography, and Cyclone Helen appeared during the splitting stage (Fig. 10).

At 1/1/00Z/08 (1/1/10L/08), the front (southeastern) part of the MJO precipitating system (clouds and precipitation) started to split into two systems and moved along the northeast and southwest coasts, while the rear (northwestern) part remained connected as shown in WRF-simulated OLR (Fig. 10a) and precipitation (Fig. 11a) fields. The southern part of the southern precipitating system appeared to interact with Cyclone Helen (2007–08)

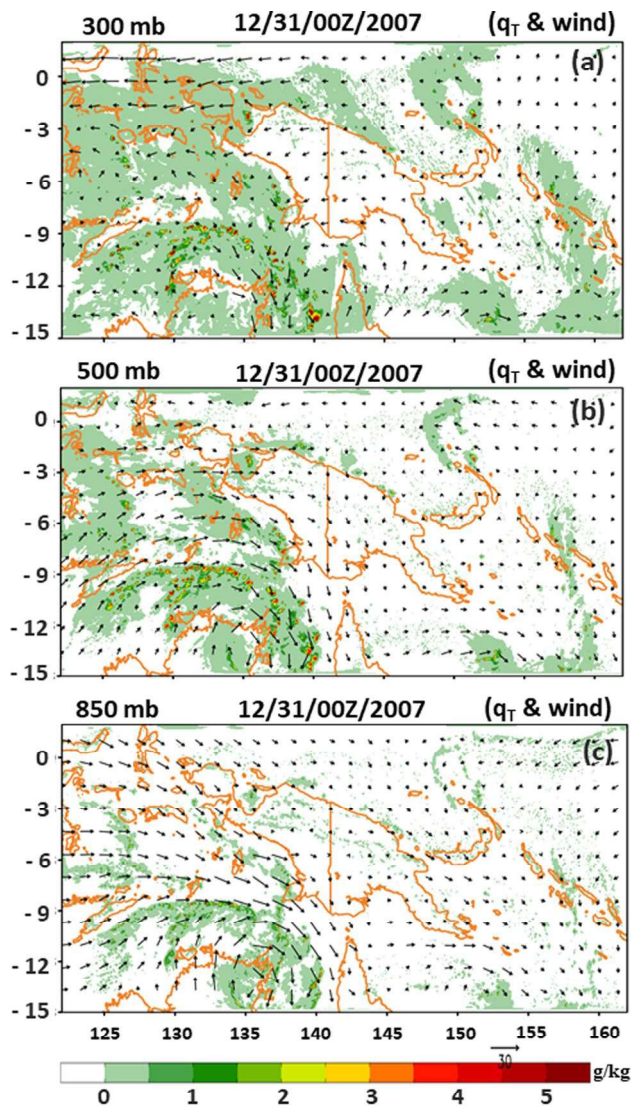


Fig. 9 (Vertical Cloud Structure-Blocking Stage) Vertical structure of the cloud (total water content) and wind fields on (a) 300 mb, (b) 500 mb, and (c) 850 mb surfaces at 12/31/00Z/07 (12/31/10L/07)

into a larger precipitating system during the period of 1/1/06Z–1/2/12Z/08 (Figs. 10b–g and 11b–g), making it difficult to distinguish these two types of clouds in the interacted region. The front end of the split precipitating systems reached the southern portion of New Guinea around 1/2/18Z/08 (Figs. 10h and 11h). Similar to the blocking stage, orographic clouds and precipitation appeared at 16L (06Z) and reached their peak around 22L (12Z) on both 1/1/08 (Figs. 10b, c and 11b, c) and 1/2/08 (Figs. 10f, g and 11f, g) caused by diurnal heating. The major differences between the model-simulated (Fig. 8) and TRMM-measured (Fig. 4) precipitation found in the blocking stage occur in the splitting stage, too.

The splitting effect of the NGH on the rainfall of MJO07–08 is further examined by analyzing the

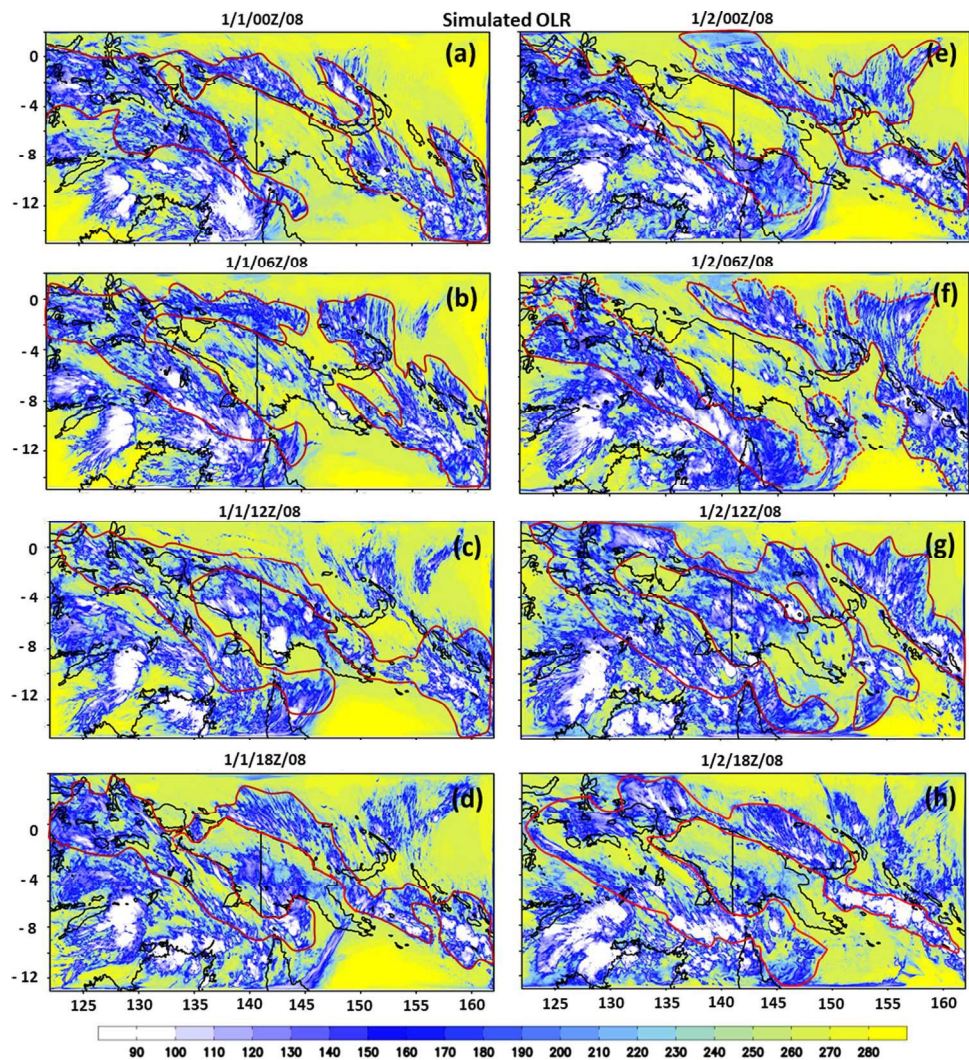
three-dimensional wind and total water content fields on 850, 500 and 300 mb surfaces (Fig. 12). The characteristics of splitting process of MJO07–08's precipitating system found in the WRF-simulated OLR and precipitation as discussed above (Figs. 10 and 11) were also shown in the cloud vertical structure (Fig. 12). These include that (a) the middle and upper tropospheric clouds were stronger, as shown at 300 mb and 500 mb (Fig. 12a, b, respectively), than those in the lower troposphere that are associated with anvil clouds associated with convection originating in the lower troposphere, and (b) the lack of clouds over New Guinea at this time (1/2/00Z/08) was because it is in the morning (10L) (Fig. 12), consistent with the rainfall fields (Fig. 11a, e).

4.3 Merging stage

The WRF-simulated OLR (Fig. 13) and precipitation (Fig. 14) fields during the merging stage (1/3/00Z/08–1/3/12Z/08) reveal that the split southern precipitating system of MJO was moving through the gap between New Guinea and Cape York Peninsula (Figs. 13a–c and 14a–c), while the northern system continued moving southeastward along the northeast coast of New Guinea. At about 1/3/18Z/08 (1/4/04L/08), there were several convective clouds and heavy rainfall areas over the ocean in between New Guinea and Cape York Peninsula (Figs. 13d and 14d). At this time, the MJO precipitating system started to split from that of Cyclone Helen. The northern and southern systems started to merge into one MJO precipitating system. This merging process is clearly depicted from the precipitation fields during 1/4/00Z and 1/4/18Z/08 (Fig. 14e–h), but not so clear in the OLR fields (Fig. 13e–h). At 1/4/18Z/08 (1/5/04L/08), the merged MJO rainfall was well organized, which then started moving southeastward (Fig. 1).

Figure 15 shows the three-dimensional structure of cloud and wind fields near the end of the splitting stage are depicted by the total water content and vector wind fields at 300 mb, 500 mb, and 850 mb at 1/4/00Z/08 (1/4/10L/08). The clouds associated with the MJO and Cyclone Helen were clearly at this time. From the cloud fields, it can be seen that the split northern and southern cloud system started to merge into one cloud system, similar to the original MJO before impinging on the NGH. Again, similar to the blocking and splitting stages, the middle and upper tropospheric clouds were stronger, as shown at 300 mb and 500 mb (Fig. 15a, b, respectively), than those in the lower troposphere that are associated with anvil clouds associated with convection originating in the lower troposphere.

Fig. 10 (WRF OLR-Splitting Stage) WRF-simulated OLR fields from 1/1/00Z/08 to 1/2/18Z/08 (1/1/10L/08–1/3/04L/08). The solid red contours denote areas with MJO deep convective clouds approximately. The orographic clouds can be seen over land



5 Concluding remarks

In this study, orographic (barrier) effects on the propagation and rainfall modification of the 2007–08 Madden–Julian Oscillation (MJO07–08) during its passage over New Guinea Highlands (NGH) are investigated by performing mesoscale analysis of outgoing longwave radiation (OLR) and precipitation fields and numerical simulation by the Advanced Research Weather Research and Forecasting (WRF) model with a single domain of 5 km grid resolution.

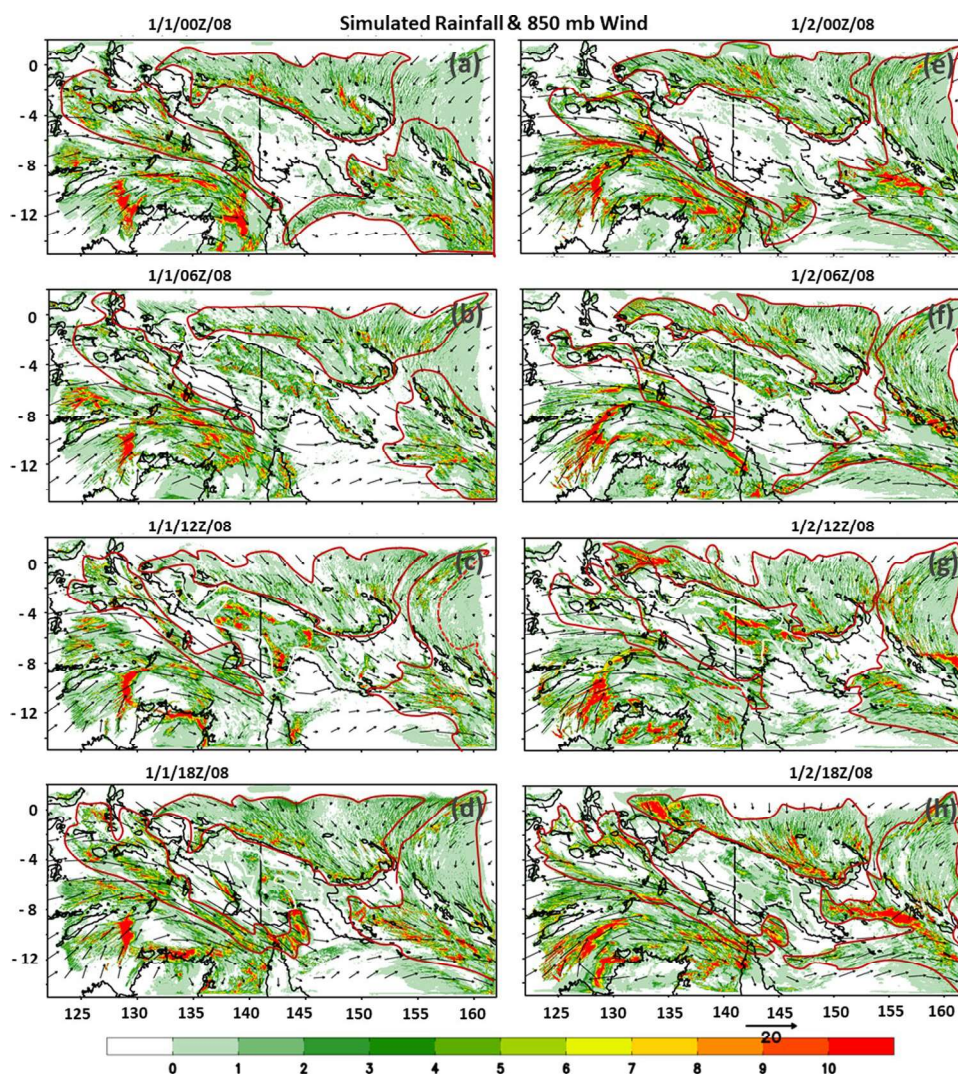
Based on the TRMM-measured rainfall and estimated OLR field and the wind field analyzed from the NCEP/NCAR Re-analysis 1 data, it is found that the *MJO precipitating system went through three distinct stages*: (1) *blocking stage* (12/30/00Z–12/31/18Z/07), (2) *splitting stage* (1/1/00Z–1/2/18Z/08), and (3) *merging stage* starting from 1/3/00Z–1/4/18Z/08 when the MJO07–08 passed over New Guinea. The WRF model results were verified by the TRMM-estimated OLR and measured rainfall fields. It was able to reproduce observed major features. They were

then used to investigate the dynamics of orographic (barrier) effect on flow and precipitating system passing over the NGH, including the three stages that MJO07–08 has gone through when it passed over New Guinea.

The blocking stage identified approximately from the TRMM-estimated OLR fields was verified much more accurately and in detail by the TRMM-measured precipitation fields. During the blocking stage (12/30–12/31/07), the incoming MJO went through three processes:

(1) From 12/31/00Z–12/31/06Z/07, the moist flow with embedded convective system of MJO0708 around A in Fig. 4e) impinged on the mountains of *northwest peninsula* of the West Papua (WIJ), which produced more rainfall over the ocean just upstream of the peninsula; (2) in the meantime, part of the incoming moist flow was forced to go around the northwest peninsula (WIJ) due to strong blocking associated with small Froude number flow passing over a three-dimensional mountain; and (3) from 12/31/12Z–12/31/18Z/07, a second blocking occurred when another moist flow impinged on the mountains of West

Fig. 11 (WRF Rain-Splitting Stage) WRF-simulated precipitation (mm) with 850 mb wind (ms^{-1}) fields from 1/1/00Z/08 to 1/2/18Z/08 (1/1/10L/08 to 1/3/04L/08). The solid red contours denote areas with heavy precipitation associated with the MJO. The orographic precipitation can be seen clearly over land



Papua, which generated or enhanced heavy rain upstream (northwest) of West Papua.

The mechanism of orographic blocking is explained by the incoming moist flow that belonged to flow-around regime, instead of flow-over regime, which was associated with low-Froude number (F_w) moist flow upstream. The F_{w1} ($=0.300$) and F_{w2} ($=0.217$) were estimated from averaging four WRF-simulated soundings upstream of the northwest peninsula (WIJ) and West Papua each, respectively, which were quite low and led to strong blocking. The strong blocking forced the flow to go around the mountains on WIJ and West Papua and MJO precipitating system to break into two systems leading to the splitting stage.

During the period of 1/1/08 to 1/2/08, it was found from the TRMM-estimated OLR fields that the MJO precipitating system approximately split into two systems with the northern and southern systems moving along the northeast and southwest coasts of NGH, respectively, toward the southeastern tip of New Guinea. Both the northern and southern

systems of the MJO precipitating system then propagated to the lee side (southeastern tip) of the mountains at a later time. Based on the TRMM-estimated OLR fields during the merging stage (1/3/00Z–1/4/00Z/08), the split MJO clouds were merging to one system around the southeastern tip. The southern precipitating system moved southeastward along the southwest coast of New Guinea in the beginning, but then strengthened and started to move eastward, which may be explained by the interaction with Cyclone Helen. At 1/4/18Z/08, these two MJO systems merged at the southeastern tip of New Guinea.

The WRF-simulated results were verified by the TRMM-estimated OLR and rainfall fields and were used to investigate the orographic effects on the propagation and rainfall modification of the MJO during its passage over the NGH. The WRF-simulated OLR fields during the blocking stage were consistent with the TRMM-estimated OLR and measured rainfall. Three types of clouds were found: (i) MJO clouds: mainly over the ocean surrounding the New Guinea,

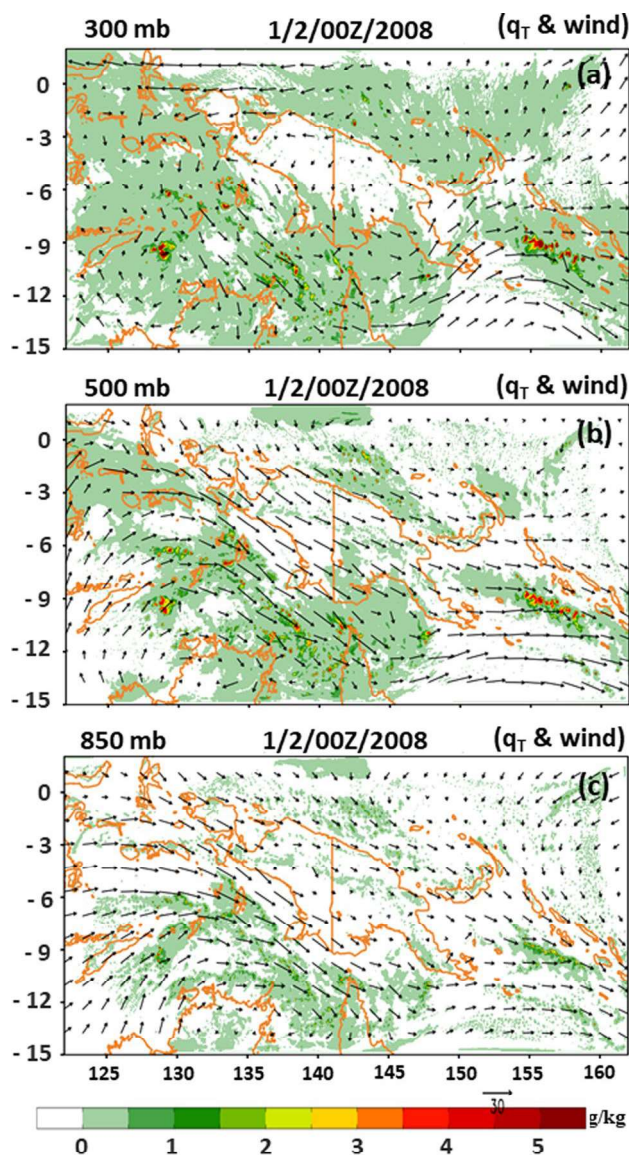


Fig. 12 (Vertical Cloud Structure-Splitting Stage) Vertical structure of the cloud (total water content) and wind fields on (a) 300 mb, (b) 500 mb, and (c) 850 mb surfaces at 1/2/00Z/08 (1/2/10L/08)

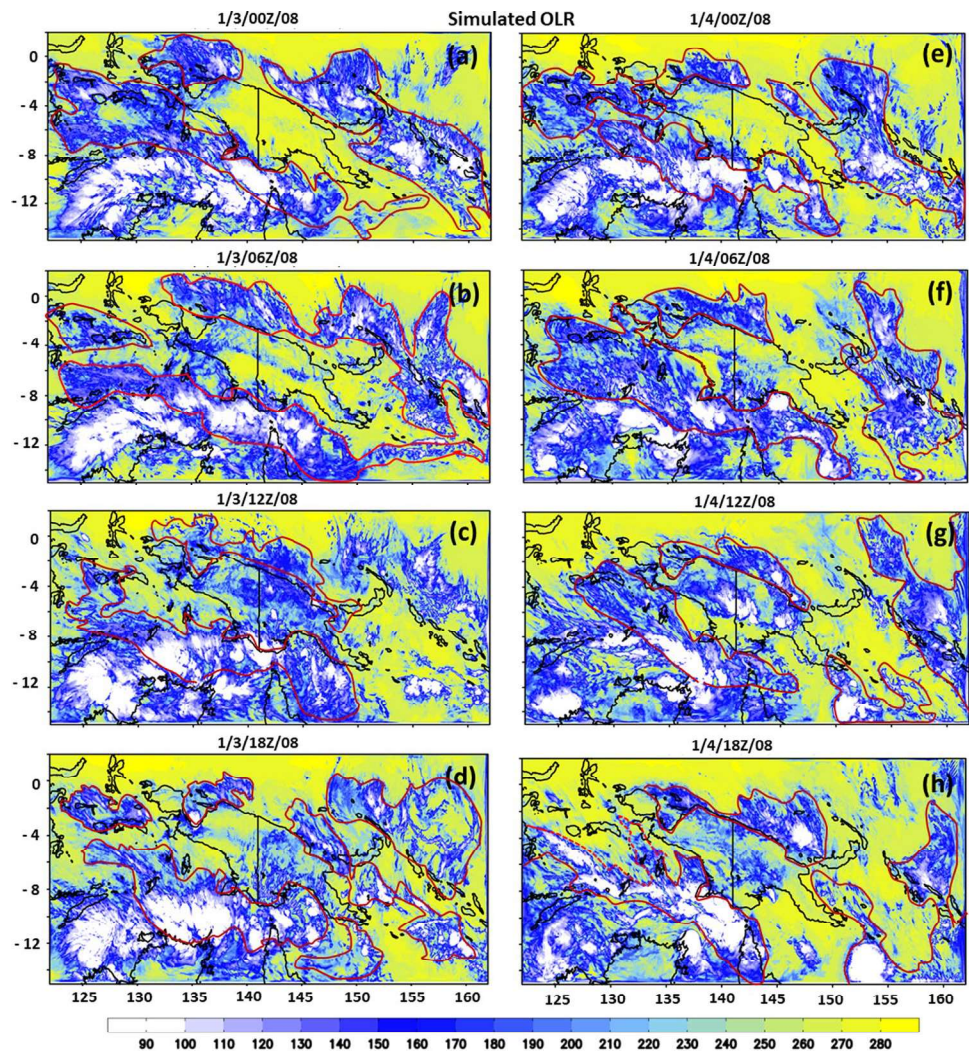
(b) orographic clouds: over land, but concentrated on NGH and surrounding areas and varied diurnally with peaks in the afternoon and evening, and (c) cyclone clouds: high and circular clouds associated with Cyclone Helen, located over the ocean. In addition to the NGH, Cyclone Helen appears to also help stall the precipitating system to the south of New Guinea. The WRF-simulated OLR fields are able to depict major features shown in observed precipitation fields, compared to the observed OLR. The lack of detailed rainfall characteristics of the TRMM rainfall appears to be caused by the coarse resolution of the TRMM data. Thus, the TRMM OLR is not appropriate to serve as proxy of the MJO rainfall, as also found in previous studies. Three types of rainfall, i.e.,

MJO, orographic, and cyclone rainfall, are well depicted by the WRF-simulated rainfall fields. The flow that went around the mountains on the northwest NGH is also shown in the 850 mb wind and precipitation fields during the blocking period. The diurnal variation of the rainfall is much more pronounced, compared to that shown in the WRF-simulated OLR fields. The major differences between the model-simulated and TRMM-measured precipitation are as follows: (a) the model-simulated rainfall area is much larger than that covered by the observed rainfall, and (b) even though they both show comparable maximum rainfall rate ($\sim 10 \text{ mm h}^{-1}$), the rainfall estimated by TRMM reveals more localized rainfall spots, which is unexpected since the WRF simulation uses a relatively fine resolution (5 km). The blocking was also revealed very well in the WRF-simulated three-dimensional wind and total water content fields on 850, 500, and 300 mb surfaces. The middle and upper tropospheric clouds were stronger than those in the lower troposphere that are associated with anvil clouds associated with convection originating in the lower troposphere.

The WRF-simulated OLR fields during the splitting stage (1/1/00Z/08–1/2/18Z/08) were able to depict cloud patterns in more detail, compared to the TRMM-estimated OLR. Similar to the blocking stage, we found that (a) the TRMM-estimated OLR was not quite accurate and is not appropriate to serve as proxy of MJO precipitation, and (b) the three types of clouds associated with the MJO, orography, and Cyclone Helen appeared during the splitting stage. It was found that the southern part of the southern precipitating system has interacted with Cyclone Helen (2007–08) into a larger precipitating system during the period of 1/1/06Z–1/2/12Z/08, making it difficult to distinguish these two types of clouds in the interacted region. Similar to the blocking stage, orographic clouds and precipitation appeared at 16L (06Z) and reached their peak around 22L (12Z) on both 1/1/08 and 1/2/08 caused by diurnal heating. The major differences between the model-simulated (Fig. 8) and TRMM-measured (Fig. 4) precipitation found in the blocking stage occur in the splitting stage too. The vertical cloud structure revealed in the WRF-simulated cloud fields during the splitting process was similar to that in the blocking stage.

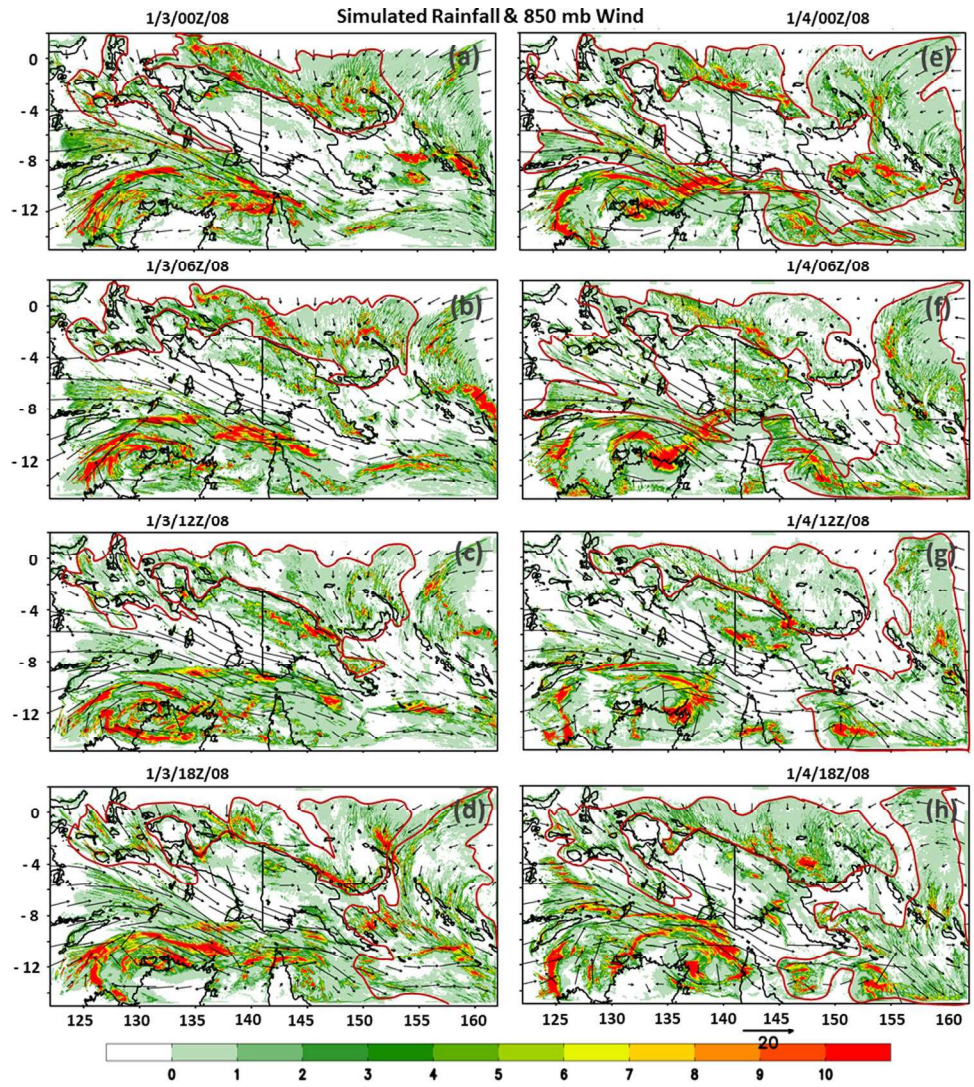
The WRF-simulated OLR and precipitation fields from 1/2/00Z/08 to 1/3/12Z/08 during the merging stage (1/3/00Z/08–1/4/18Z/08) reveal that the split southern precipitating system of MJO was moving through the gap

Fig. 13 (WRF OLR-Merging Stage) WRF-simulated OLR from 1/3/00Z/08 to 1/4/18Z/08 (1/3/10L/08–1/5/04L/08). The solid red contours denote areas with MJO deep convective clouds approximately. The orographic clouds can be seen over land at 06Z (16L) and 12Z (22L) in both days



between New Guinea and Cape York Peninsula, while the northern system continued moving southeastward along the northeast coast of New Guinea. At about 1/3/18Z/08, the northern and southern systems started to merge into one MJO precipitating system. This merging process is clearly depicted from the precipitation fields from 1/4/00Z/08 to 1/4/18Z/08, but not so clear in the OLR fields (Fig. 13e–h). At 1/4/18Z/08 (1/5/04L/08), the merged MJO rainfall was well organized, which then started moving southeastward. The vertical cloud structure revealed in the WRF-simulated cloud fields during the merging process was similar to that in the blocking and splitting stages.

Fig. 14 (WRF Rain-Merging Stage) WRF-simulated precipitation (mm) with 850 mb wind (ms^{-1}) fields from 1/3/00Z/08 to 1/4/18Z/08 (1/3/10L/08–1/5/04L/08). The solid red contours denote areas with heavy precipitation associated with the MJO. The orographic precipitation can be seen clearly over land at 06Z (16L) and 12Z (22L) in both days



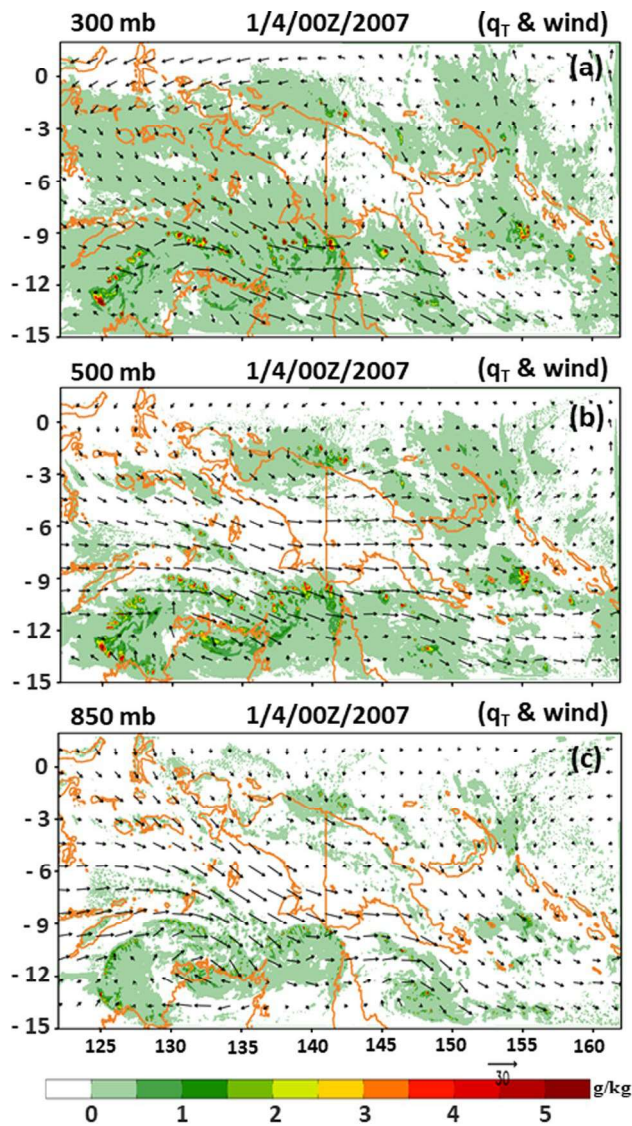


Fig. 15 (Vertical Cloud Structure-Merging Stage) Vertical structure of the cloud (total water content) and wind fields on (a) 300 mb, (b) 500 mb, and (c) 850 mb surfaces at 1/4/00Z/08 (1/4/10L/08)

Acknowledgements The authors would like to acknowledge Drs. J. Zhang, A. Mekonnen, and L. Liu at the North Carolina A&T State University for their insightful discussions and comments on this paper. This research was supported by the National Science Foundation Award AGS-1265783, HRD-1036563, OCI-1126543, and CNS-1429464.

References

- Chang SWJ (1982) The orographic effects induced by an island mountain range on propagating tropical cyclones. *Mon Wea Rev* 110:1255–1270. [https://doi.org/10.1175/1520-0493\(1982\)110,1255:TOEIBA.2.0.CO;2](https://doi.org/10.1175/1520-0493(1982)110<1255:TOEIBA.2.0.CO;2)
- Chen SH, Lin YL (2005) Orographic effects on a conditionally unstable flow over an idealized three-dimensional mesoscale unstable

mountain. *Meteorol Atmos Phys* 88:1–21. <https://doi.org/10.1007/s00703-017-0557-2>

- Chu CM, Lin YL (2000) Effects of orography on the generation and propagation of mesoscale convective systems in a two-dimensional conditionally unstable flow. *J Atmos Sci* 57:3817–3837. [https://doi.org/10.1175/1520-0469\(2001\)057<3817:EOOOTG>2.0.CO;2](https://doi.org/10.1175/1520-0469(2001)057<3817:EOOOTG>2.0.CO;2)
- Emanuel KA (1994) *Atmospheric convection*. Oxford University Press, New York
- Epifano CC (2003) Lee vortices. *Encyclo Atmos Sci*. Cambridge Univ Press, Cambridge
- Glickman TS (2000) *Glossary of Meteorology*, 2nd edn. American Meteorology Society, Boston
- Gottschalck J, Zhang Q, Wang W, L'Heureux M, Peng P (2008) MJO monitoring and assessment at the Climate Prediction Center and initial impressions of the CFS as an MJO forecast tool. NOAA CTB–COLA Joint Semin 15–22. https://www.nws.noaa.gov/ost/climate/STIP/CTB-COLA/Jon_042308.pdf. Accessed 1 July 2019
- Hong S-Y, Lim J-OJ (2006) The WRF single-moment 6-class microphysics scheme (WSM6). *J Korean Meteor Soc* 42:129–151
- Hsu HH, Lee MY (2005) Topographic effects on the eastward propagation and initiation of the Madden–Julian oscillation. *J Clim* 18:795–809. <https://doi.org/10.1175/JCLI-3292.1>
- Huffman GJ, Bolvin DT, Nelkin EJ, Wolff DB, Adler RF, Gu G, Hong Y, Bowman KP, Stocker EF (2007) The TRMM multisatellite precipitation analysis (TMPA): quasi-global, multiyear, combined-sensor precipitation estimates at fine scales. *J Hydro-meteor* 8(1):38–55
- Inness PM, Slingo JM (2006) The interaction of the Madden–Julian oscillation with the maritime continent in a GCM. *Q J R Meteorol Soc* 132:1645–1667. <https://doi.org/10.1256/qj.05.102>
- Jiang LC (2012) The interaction between the MJO and topography: Using high resolution data. Master Thesis, Department of Atmospheric Sciences, National Taiwan University, 82pp
- Kim D, Kim H, Lee MI (2017) Why does the MJO detour the maritime continent during austral summer? *Geophys Res Lett* 44:2579–2587. <https://doi.org/10.1002/2017GL072643>
- Lin YL (2007) *Mesoscale dynamics*. Cambridge University Press, Cambridge
- Lin YL, Chen SH, Liu L (2016) Orographic effects on track deflection of an idealized tropical cyclone passing over a mesoscale mountain range. *J Atmos Sci* 73:3951–3974. <https://doi.org/10.1175/JAS-D-15-0252.1>
- Ling J, Zhang C, Joyce R, Xie P-P, Chen G (2019) Possible role of the diurnal cycle in land convection in the barrier effect on the MJO by the maritime continent. *Geophys Res Lett* 46:3001–3011. <https://doi.org/10.1029/2019GL081962>
- Matthews AJ, Pickup G, Peatman SC, Clews P, Martin J (2013) The effect of the Madden–Julian oscillation on station rainfall and river level in the fly river system, Papua New Guinea. *J Geophys Res Atmos* 118:10926–10935. <https://doi.org/10.1002/jgrd.50865>
- Monier E, Weare BC, Gustafson WI (2010) The Madden–Julian oscillation wind-convection coupling and the role of moisture processes in the MM5 model. *Clim Dyn* 35:435–447. <https://doi.org/10.1007/s00382-009-0626-4>
- Peatman SC, Matthews AJ, Stevens DP (2014) Propagation of the Madden–Julian oscillation through the maritime continent and scale interaction with the diurnal cycle of precipitation. *Q J R Meteorol Soc* 140:814–825. <https://doi.org/10.1002/qj.2161>
- Rauniyar SP, Walsh KJE (2013) Influence of ENSO on the diurnal cycle of rainfall over the maritime continent. *J Climate* 26:1304–1321. <https://doi.org/10.1175/JCLI-D-12-00124.1>
- Simpson J, Kummerow C, Tao WK, Adler RF (1996) On the tropical rainfall measuring mission (TRMM). *Meteorol Atmos Phys* 60(1):19–36

- Skamarock WC, Klemp JB, Dudhia J, Gill DO, Barker DM, Duda MG, Huang XY, Wang W, Powers JG (2008) A description of the advanced research WRF version 3. NCAR Tech Note. https://www.mmm.ucar.edu/wrf/users/docs/arw_v3.pdf. Accessed 7 Mar 2016
- Smith RB (1989) Hydrostatic airflow over mountains *Adv Geophys* 31:1–41
- Smolarkiewicz PK, Rotunno R (1989) Low Froude number flow past three-dimensional obstacles. Part I: Baroclinically generated lee vortices. *J Atmos Sci* 46:1154–1164. [http://doi.org/10.1175/1520-0469\(1989\)046<1154:LFNFPT>2.0.CO;2](http://doi.org/10.1175/1520-0469(1989)046<1154:LFNFPT>2.0.CO;2)
- Tseng W-L, Hsu H-H, Keenlyside N, Chang C-WJ, Tsuang B-J, Tu C-Y, Jiang L-C (2017) Effects of surface orography and land-sea contrast on the Madden-Julian oscillation in the maritime continent: a numerical study using ECHAM5-SIT. *J Clim* 30:9725–9741. <https://doi.org/10.1175/JCLI-D-17-0051.1>
- Wikipedia (2018) Cyclone Helen (2008). [https://en.wikipedia.org/wiki/Cyclone_Helen_\(2008\)](https://en.wikipedia.org/wiki/Cyclone_Helen_(2008)). Accessed 23 May 2018
- Wu CH, Hsu HH (2009) Topographic influence on the MJO in the Maritime Continent. *J Clim* 22:5433–5448. <https://doi.org/10.1175/2009JCLI2825.1>
- Zhang C, Ling J (2017) Barrier Effect of the Indo-Pacific maritime continent on the MJO: perspectives from tracking MJO Precipitation. *J Clim* 30:3439–3459. <https://doi.org/10.1175/JCLI-D-16-0614.1>

Publisher's Note Springer Nature remains neutral with regard to jurisdictional claims in published maps and institutional affiliations.

Terms and Conditions

Springer Nature journal content, brought to you courtesy of Springer Nature Customer Service Center GmbH (“Springer Nature”).

Springer Nature supports a reasonable amount of sharing of research papers by authors, subscribers and authorised users (“Users”), for small-scale personal, non-commercial use provided that all copyright, trade and service marks and other proprietary notices are maintained. By accessing, sharing, receiving or otherwise using the Springer Nature journal content you agree to these terms of use (“Terms”). For these purposes, Springer Nature considers academic use (by researchers and students) to be non-commercial.

These Terms are supplementary and will apply in addition to any applicable website terms and conditions, a relevant site licence or a personal subscription. These Terms will prevail over any conflict or ambiguity with regards to the relevant terms, a site licence or a personal subscription (to the extent of the conflict or ambiguity only). For Creative Commons-licensed articles, the terms of the Creative Commons license used will apply.

We collect and use personal data to provide access to the Springer Nature journal content. We may also use these personal data internally within ResearchGate and Springer Nature and as agreed share it, in an anonymised way, for purposes of tracking, analysis and reporting. We will not otherwise disclose your personal data outside the ResearchGate or the Springer Nature group of companies unless we have your permission as detailed in the Privacy Policy.

While Users may use the Springer Nature journal content for small scale, personal non-commercial use, it is important to note that Users may not:

1. use such content for the purpose of providing other users with access on a regular or large scale basis or as a means to circumvent access control;
2. use such content where to do so would be considered a criminal or statutory offence in any jurisdiction, or gives rise to civil liability, or is otherwise unlawful;
3. falsely or misleadingly imply or suggest endorsement, approval, sponsorship, or association unless explicitly agreed to by Springer Nature in writing;
4. use bots or other automated methods to access the content or redirect messages
5. override any security feature or exclusionary protocol; or
6. share the content in order to create substitute for Springer Nature products or services or a systematic database of Springer Nature journal content.

In line with the restriction against commercial use, Springer Nature does not permit the creation of a product or service that creates revenue, royalties, rent or income from our content or its inclusion as part of a paid for service or for other commercial gain. Springer Nature journal content cannot be used for inter-library loans and librarians may not upload Springer Nature journal content on a large scale into their, or any other, institutional repository.

These terms of use are reviewed regularly and may be amended at any time. Springer Nature is not obligated to publish any information or content on this website and may remove it or features or functionality at our sole discretion, at any time with or without notice. Springer Nature may revoke this licence to you at any time and remove access to any copies of the Springer Nature journal content which have been saved.

To the fullest extent permitted by law, Springer Nature makes no warranties, representations or guarantees to Users, either express or implied with respect to the Springer nature journal content and all parties disclaim and waive any implied warranties or warranties imposed by law, including merchantability or fitness for any particular purpose.

Please note that these rights do not automatically extend to content, data or other material published by Springer Nature that may be licensed from third parties.

If you would like to use or distribute our Springer Nature journal content to a wider audience or on a regular basis or in any other manner not expressly permitted by these Terms, please contact Springer Nature at

onlineservice@springernature.com